International Journal of Engineering & Technology, 9 (3) (2020) 804-811

International Journal of Engineering & Technology

Website: www.sciencepubco.com/index.php/IJET

Research paper

Thermal performance for electromagnetohydrodynamic flow of non-Newtonian Casson fluid through porous microtube

Motahar Reza [1, 2 *], Amalendu Rana1 [1, 2, 3], Raghunath Patra [3]

[1] *Department of Mathematics, GITAM University, Hyderabad, India*
[2] *Department of Mathematics, National Institute of Science and Technology, Berhampur, India*
[3] *Department of Mathematics, Berhampur University, Berhampur-760007, Odisha, India*
**Corresponding author E-mail: motaharreza90@gmail.com*

Abstract

A theoretical investigation is done to analyze the heat transfer features of non-Newtonian Casson fluid in a porous microtube with electro kinetic effects associated with the applied magnetic field. The exact analytical solutions the velocity and temperature profiles of non-Newtonian Casson fluid in porous micro-tube related to combining effects of electromagnetohydrodynamics forces and electrokinetic forces have been obtained using a variation of parameter. Temperature and flow distribution characteristics of Casson fluid flow are controlled by the obtruded pressure-gradients, applied a magnetic field and electro-kinetic forces. The exciting features of the electromagnetohydrodynamics flow along with the features of the heat flow rate are examined by variation in the non-dimensional physical arguments on velocity and temperature functions. The effect of the Casson parameter on the velocity and temperature profiles has been investigated analyzed. The fluid flow rate and the heat transfer rate of Casson fluid within porous micro-tube is controlled by the strength applied electric and magnetic field.

Keywords: *Electromagnetohydrodynamic Flow; Microtube; Porous Medium; Casson Fluid.*

1. Introduction

To design an efficient small scale system, microfluidics is used in many applications which involves heat and mass transfer characteristics, separation, detection, and analysis of blood, proteins, food, etc. in micro-organs of living animals or plants. Electrokinetics flows such as Electroosmosis have gained interest as the mechanism for ascertaining fluid flows in microdevices instead of pressure-driven and other flow mechanisms because of the accuracy and other benefits associated with this kind of arrangement [1-2]. Although it is observed from many applications regarding the upper limit of the strength of the lateral component of electric force, But it can also be employed for the flow in a microchannel or micro-tube to bound the Joule Heating effectuates and linked negative consequences[5,6]. For further experiments, it was found that the flows in microchannels can be augmented by using the combined effects of electromagnetohydrodynamics (EMHD) and it was also experimentally [7] found that the standard flow rates in microchannels can be considerably increased by using minimum strength of the magnetic field. Two-phase flow in a porous or non-porous microchannel in the presence of a magnetic field is studied by Chamkha et al. [8] [9]. The brief review of the experimental and simulation work for industrial applications of nanofluid flow in various geometry of microchannel has been discussed by Chamkha et al. [10]. Unsteady natural convection in a porous channel in the presence of a magnetic field has been studied by Chamkha [11]. The combined effect of the magnetic field and heat generation on non-Darcy mixed convection flow through a porous medium channel has been analyzed by Chamkha [12].

Last few decades, a number of researchers are working on MHD convection flow in the porous medium which has a wide range application in the field of industrial Engineering and biomedical instruments [14]-[15]. Design of MHD power generator, nuclear waste processing, and distribution of chemical waste control, blood flow in micro-channel as an application for lab-on-a-chip (LOC). Many bio-medical devices work based on the principle of peristaltic or MHD pumping for the transportation of fluids without internal moving parts, for example, blood in the heart-lung machine. Recently scientists are showing interest to investigate the mechanical and physiological properties of blood flow in human arteries. Human blood is also modeled as Casson fluid. The non-Newtonian behavior of blood in a stenosed artery over the plaque is considered as Casson fluid flow in a porous medium (Buchanan et al.,[16]; Chakravarty [17]; Cho and Kensey [18]). Plaques are often recognized to be porous (Ku[19]). Thus their porosity is considered in any important analysis for having more realistic results. (Dash et al., [20]). This type of model also is examined in the presence of a magnetic field for other different applications, like drug delivery, MHD therapy, etc.

In most of the technology, transport of non-Newtonian fluid through microchannel is found and this transport mechanism is characterized by mathematically considering the material behavior on non-linear relation between stress and strain-rate. The constitutive model is essential to describe the physical material properties. Recently, many mathematical models have been studied by many researchers [21-22] to analyze the non-Newtonian characteristic. Liu and Yang [21] invested the two-phase flow of blood cells in the microvascular network using electroosmotic force. Liu et. Al [22] have analyzed the numerical scheme on two-phase bio-fluid in a micro device using electrokinetic force. Ng [23] studied the flow rate of Casson fluid in microchannel governed by the electroosmotic (EO) and pressure force. The effect of electrokinetic and interfacial slip on thermal transport of electromagnetohydrodynamics (EMHD) flow in microtube is studied by Chen et. al. [24]. Features of temperature function of fluid flow in porous circular microtube are examined by Wang et al. [25]. Afonso et al. [26] performed an analytical investigation of the electroosmotic flow of two viscoelastic fluid. A comprehensive analysis of heat transfer of nano-fluid through a microtube under the streaming potential effects is done by Zhao et al [27]. Jian [28] investigated the transient MHD heat transfer and entropy generation through a micro parallel channel with combined electroosmotic effects and pressure gradient. Thermal characteristics of an EMHD flow through microchannel under constant wall heat flux conditions are analyzed by Chakraborty et al. [29]. The objective of this investigation is to study the features of momentum and heat transport for Casson fluid flow in porous microtube under electrokinetic force associated with pressure and magnetic energy. The exact analytical solutions of velocity and temperature functions for the Casson fluid flow are derived using the variation of parameter. The transport phenomenon of this fluid flow has been examined under the combined effect of the electric double layer and applied magnetic field as well as an electric force. The features of the electromagnetohydrodynamics (EMHD) flow along with heat transfer characteristics are investigated by variation in the non-dimensional flow velocity and temperate profiles. The effect of the Casson parameter and strength of the magnetic parameter (Ha) on the velocity and temperature distribution has been examined and analyzed.

2. Mathematical modeling and problem description

The EMHD flow of a Casson fluid in microtube under the electrokinetic force is considered along the axial direction of the microtube. The physical sketch of this flow problem is depicted in Fig 1. This circular microtube is replete by a porous medium where R and L denote the radius of the microtube and length of the microtube respectively. In the radial direction, the electromagnetic field is induced by the applied magnetic field and electric field. The polar, cylindrical coordinate (r, θ, z) is considered to describe the governing equations of this flow problem.

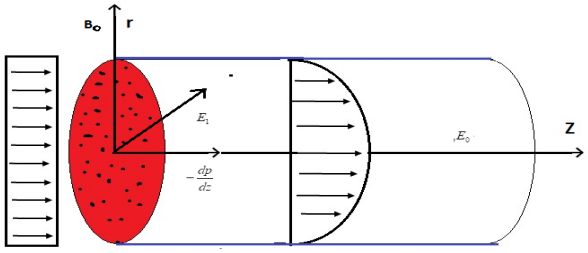

Fig. 1 : Schematic Diagram of Circular Microtube with Porous Medium.

In this flow problem Casson- nanofluid is considered where the base fluid is the non-Newtonian Casson fluid. The Casson fluid sample plays Newtonian and non-Newtonian both fluid behavior. The constitutive equation for Casson fluid model [20] can be followed by

$$\tau_{ij} = \begin{cases} \left(\mu_c + \frac{P_s}{\sqrt{2\pi}}\right) 2e_{ij}, \pi > \pi_0 \\ \left(\mu_c + \frac{P_s}{\sqrt{2\pi_0}}\right) 2e_{ij}, \pi < \pi_0 \end{cases} \quad (1)$$

where the yield stress of the fluid is $P_s = e_{ij}e_{ij}$ and e_{ij} indicates the deformation rate at (i, j) th component. π is the product of the component of deformation rate with itself, π_0 is a critical value of this product based on the non-Newtonian fluid model, μ_c represents the plastic dynamic viscosity of the non-Newtonian fluid. Then from (1) it is obtained that (for $\pi < \pi_0$)

$$\tau_{ij} = \mu_c \left(1 + \frac{1}{\beta}\right) 2e_{ij} \quad (2)$$

Where $\beta = \mu_c\sqrt{2\pi_0}/P_s$ is the Casson parameter.

2.1. Potential distribution within EDL

In electroosmotic flow, to derive the net charge density ρ_e inside the EDL, first, the EDL potential ψ is found out by solving the Poisson–Boltzmann equation:

$$\nabla.(\nabla\psi) = -\frac{\rho_e}{\varepsilon} \quad (3)$$

Where ε denotes the permittivity of the conducting Casson fluid. The relationship among the charge density ρ_e and the electric potential ψ is established by

$$\rho_e = -2n_0 ez \sinh\left(\frac{ez\psi}{k_B T}\right) \quad (4)$$

Where e denotes the electronic charge, z represents the valence, $k_B$is the Boltzmann constant, the ion density $n_0 = \frac{\varepsilon k_B T}{8\pi e^2 z^2 \lambda^2}$, and T is the local temperature. Since ψ is small enough, so $(ez\psi/k_B T) << 1$, the term $\sinh(ez\psi/k_B T)$ can be approximated by $(ez\psi/k_B T)$. This principle is known as Dybye-Hückle linearization. [26,27,28]. The EDL potential distribution function can be assumed the function of the radial direction only, i.e.$\psi = \psi(r)$. Hence the EDL potential distribution can be obtained as:

$$\frac{1}{r}\frac{\partial}{\partial r}\left(\frac{\partial^2 \psi}{\partial r^2}\right) = \kappa^2 \psi \tag{5}$$

Where $\kappa = ez\left(\frac{2n_0}{\varepsilon k_B T}\right)^{\frac{1}{2}}$ is Dybye-Hückle parameter and $1/\kappa$ be the thickness of the EDL. And the boundary conditions are

$$\psi = \psi_w \text{ at } r = R, \frac{\partial \psi}{\partial r} = 0 \text{ at } r = 0. \tag{6}$$

Here ψ_w be the wall zeta potential. We obtain easily the analytical EDL potential distribution in cylindrical coordinate system

$$\psi = \psi_w I_0(\kappa r)/I_0(\kappa R) \tag{7}$$

We introduce the non-dimensional variables $\psi^* = \psi(ez/k_B T)$, $\psi_w^* = \psi_w(ez/k_B T)$ $r^* = r/R$, $k = \kappa R$ to make dimensionless the expressions of equation (7) can be represented by

$$\psi^* = \psi_w^* I_0(kr^*)/I_0(k) \tag{8}$$

where k is called the normalized reciprocal thickness of the EDL which representing the ratio of half-height of the microchannel to Debye length (i.e. $1/\kappa$).And I_0 is the modified Bessel function of the first kind with zero order.

2.2. Governing equations and velocity distribution analysis

The incompressible viscous flow problem which is also affected by the combined effect of electromagnetohydrodynamic force through microtube through a porous medium is considered. The governing equations for the flow of the electrolyte solute can be expressed, as follows:

$$\frac{\partial \rho}{\partial t} + \nabla.\left(\rho \vec{V}\right) = 0 \tag{9}$$

$$\frac{D}{Dt}\left(\rho \vec{V}\right) = \nabla.(\vec{\tau}) + \vec{b} \tag{10}$$

Where ρ represents the density of Casson fluid and $\vec{V}$ denotes the velocity of this fluid, $\vec{b}$ is the body force which is the combined effect of electro-kinematic and magnetic force so that it can be written as :

$$\vec{b} = \rho_e \vec{E} + \vec{F}, \tag{11}$$

Here the total electric charge density is ρ_e , the imposed electric field is $\vec{E} = (E_1, 0, E_0)$ and due to external magnetic force, there exist Lorentz force $\vec{F}$ which can be expressed as

$$\vec{F} = \vec{J} \times \vec{B} \tag{12}$$

$\vec{B} = (B_o, 0,0)$ is applied magnetic field and σ_e is called the electrical conductivity and $\vec{J} = \sigma_e(\vec{E} + \vec{u} \times \vec{B})$. The flow problem is considered a fully developed flow under the cylindrical coordinate system. The simplified form of the momentum conservation equation along the z-direction, assuming a hydrodynamically fully developed flow of a non-Newtonian Casson fluid is written as:

$$\left(1 + \frac{1}{\beta}\right)\left(\frac{d^2u}{dr^2} + \frac{1}{r}\frac{du}{dr}\right) - \frac{\mu}{K}u - \frac{dp}{dz} + \rho_e E_0 + \sigma_e B_0 E_1 - \sigma_e B_0^2 u = 0 \tag{13}$$

where β is the Casson parameter, K denoted the permeability of the porous medium and E_0 is the axial component and E_1 is the lateral transverse component of applied electrical force. Due to the small ratio of the diameter and length of the microtube, although the body force may exist in the radial or angular direction and the velocity in these directions is much smaller than the axial direction [29]. Therefore only one momentum equation is considered in the axial direction. The boundary conditions are derived as follows:

$$u(r = R) = 0\,, \frac{du}{dr}(r = 0) = 0 \tag{14}$$

Let us introduce the following dimensionless variables and parameters:

$$u^* = \frac{u}{U}\,, r^* = \frac{r}{R}\,, G = \frac{R^2\left(\frac{dp}{dz}\right)}{\mu U}\,, Da = \frac{K}{R^2}\,, S = \frac{E_1}{UB_0}\,, Ha = B_0 R\sqrt{\frac{\sigma_e}{\mu}}\,, U = \frac{E_0 \varepsilon k_b T}{ez\mu}$$

Where U be the reference velocity, G be the non-dimensional pressure gradient. Ha is the Hartmann number which is indicating the strength of the applied magnetic field B_0 and Da is the Darcy number. S represents the strength of the transverse electric E_1 field. The non-dimensional form of the equation (12) is reduced by:

$$\left(1+\frac{1}{\beta}\right)\left(\frac{d^2u^*}{dr^{*2}}+\frac{1}{r^*}\frac{du^*}{dr^*}\right)-\left(\frac{1}{Da}+Ha^2\right)u^*+k^2\psi_w^*\frac{I_0(kr^*)}{I_0(k)}+Ha^2S-G=0 \tag{15}$$

Boundary condition (13) is reduced as follows:

$$u^*(1)=0;\ \frac{du^*}{dr^*}=0\ at\ r^*=0. \tag{16}$$

Equation (15) is analytically solved analytically based the boundary conditions (16) to obtain the exact solutions which are written as

$$u(r^*)=\frac{I_0\left(\sqrt{\frac{\frac{1}{Da}+Ha^2}{1+\frac{1}{\beta}}}\,r^*\right)}{I_0\left(\sqrt{\frac{\frac{1}{Da}+Ha^2}{1+\frac{1}{\beta}}}\right)}\left\{\frac{k^2\psi_w^*\left(\frac{1}{Da}+Ha^2\right)}{\left(1+\frac{1}{\beta}\right)\left(\frac{\frac{1}{Da}+Ha^2}{1+\frac{1}{\beta}}-k^2\right)}+\frac{G-Ha^2S}{1+\frac{1}{\beta}}\right\}-\frac{G-Ha^2S}{1+\frac{1}{\beta}}-\frac{k^2\psi_w^*\left(\frac{1}{Da}+Ha^2\right)}{\left(1+\frac{1}{\beta}\right)\left(\frac{\frac{1}{Da}+Ha^2}{1+\frac{1}{\beta}}-k^2\right)}\frac{I_0(kr^*)}{I_0(k)} \tag{17}$$

The above expression of velocity function depends on different physical parameters like Hartmann number Ha, Casson parameter β, Darcy number Da, etc.

2.3. Temperature distribution and heat transfer analysis

The governing equation for thermally fully developed flow is expressed as:

$$\frac{D}{Dt}(\rho C_P T)=\nabla.(k_{Th}\nabla T)+\vec{\tau}\vec{D}+\dot{q} \tag{18}$$

Where $\vec{D}$ is the strain rate tensor k_{Th} be the thermal conductivity of the fluid, and $\dot{q}$ is the heat generation per unit volume due to joule heating, given by

$$\dot{q}=\frac{(\rho_e\vec{V}+\sigma\vec{E})\,(\rho_e\vec{V}+\sigma\vec{E})}{\sigma}$$

Here σ is the electric conductivity of the fluid. To investigate the thermal transport characteristics associated with electro-magnetohydro-dynamic flows through a circular microtube by considering volumetric heat generation terms Joule heating in the cylindrical coordinate system can be written as:

$$\rho C_P u\frac{\partial T}{\partial z}=k_{Th}\left\{\frac{1}{r}\frac{\partial}{\partial r}\left(r\frac{\partial T}{\partial r}\right)+\frac{\partial^2T}{\partial z^2}\right\}+S_J \tag{19}$$

Where C_p the specific heat of the liquid at constant pressure, T is is the local temperature of the liquid, k_{Th} is the thermal conductivity of the liquid, and $S_J=\sigma(E_1^2+E_0^2)$ is the volumetric heat generation [30] due to Joule heating effect. We consider the constant wall heat flux boundary condition on the wall and we have $\frac{\partial T_w}{\partial z}=\frac{\partial T_m}{\partial z}=\frac{\partial T}{\partial z}=constant$ and $\frac{\partial^2T}{\partial z^2}=0$. where T_w and T_m are the local walls and bulk mean temperature. The overall energy balance on an elemental control volume yields

$$\frac{\partial T_m}{\partial z}=\frac{2\pi Rq_w+\sigma_eS_J\pi R^2}{\rho C_pu_m\pi R^2} \tag{20}$$

where u_m is the axial mean velocity, which can be expressed as

$$u_m=\frac{\int_0^{2\pi}\int_0^R urdrdz}{\pi R^2} \tag{21}$$

To reduce the energy equation in a dimensionless form, we introduce the suitable non-dimensional temperature $\theta=(T-T_w)/(\frac{q_wR}{k_{Th}})$. Then the dimensionless energy equation and can be written as:

$$\frac{1}{r^*}\frac{\partial}{\partial r^*}\left(r^*\frac{\partial\theta}{\partial r^*}\right)=\left(1+\frac{S_1}{2}+\frac{Ha^2BrS^2}{2}\right)\frac{u}{\beta_1}-S_1 \tag{22}$$

Where $S_1=\frac{S_JR}{q_w}$, $Br=\frac{\mu U^2}{q_wR}$, $\beta_1=\int_0^1u^*r^*dr^*$. Here S_1 is the ratio of joule heating which is a dimensionless joule heating parameter. Br is the Brinkman number.
Boundary conditions are given by:

$$\theta(r^*=1)=0\,,\frac{d\theta}{dr^*}(r^*=0)=0 \tag{23}$$

The analytical expression of the temperature distribution is derived and written as

$$\theta=F(r^*)-F(1) \tag{24}$$

$F(1)$ is the functional value of the function $F(r^*)$ at $r^*=1$. where?

$$F(r^*) = \int \frac{1}{r^*}\left(\int r^* \left\{\left(1 + \frac{S_1}{2} + \frac{Ha^2 BrS^2}{2}\right)\frac{u^*}{\beta_1} - S_1\right\} dr^*\right) dr^* \tag{25}$$

According to the obtained temperature distribution and velocity distribution, the non-dimensional bulk temperature can be written by the following expression:

$$\tilde{\theta} = \frac{\int_0^{2\pi}\int_0^1 u^*\theta r^* dr^* dz}{\int_0^{2\pi}\int_0^1 u^* r^* dr^* dz} = \frac{k_{Th}(T_w - T_m)}{Rq_w} \tag{26}$$

In thermal transport phenomenon an important heat transfer parameter can be expressed as Nusselt number Nu, which illustrates the rate of heat transfer and can be defined as:

$$Nu = \frac{2Rq_w}{k_{Th}(T_w - T_m)} = -\frac{2}{\tilde{\theta}} \tag{27}$$

3. Results and discussion

The velocity and temperature distribution of the Casson fluid in a porous microtube under electrokinetic force associated with applied magnetics energy has been examined. The interesting part is to be noted from this analysis that the governing equations of the mathematical model for this flow problem have been solved analytically using a variation of parameter. The exact solutions for the velocity and temperature distribution of the non-Newtonian Casson fluid flow inside the EDL are analyzed by variation of the physical parameters associated with the combined effect of Hartman number (Ha) and lateral transverse electric field(S).

To validate the present computed results, we compare the velocity profile with the results of Chen et al. [24]. They (Chen et al. [24]) examined the pressure-driven flow through a microtube with the EMHD effect with interfacial boundary conditions. When the slip parameter is equal to zero, then the boundary condition becomes a no-slip boundary condition. It can be observed from Fig. 2 that the present results for the velocity distribution show an excellent agreement with the analytical solutions by Chen et al. [24] when the slip parameter is ignored. Further, we discuss the results of present results of flow velocity and temperature distribution with the influences of the magnetic field, transverse electric field, Casson parameter, and Darcy number.

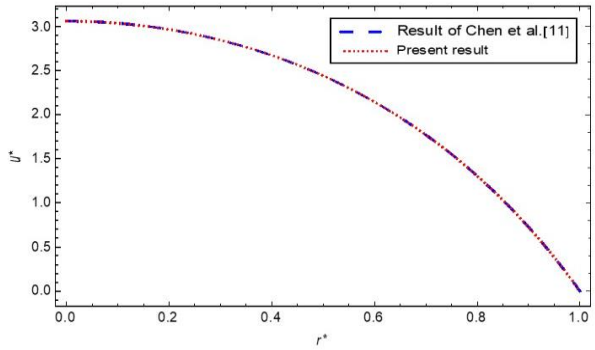

Fig. 2: Comparison of the Present Analytical Solution of Velocity Distribution with the Result of Chen Et Al. [24] ($\Psi_w^* = -1, G = -1, Ha = 1, S = 10, k = 4, \frac{1}{\beta} = 0, \frac{1}{Da} = 0$).

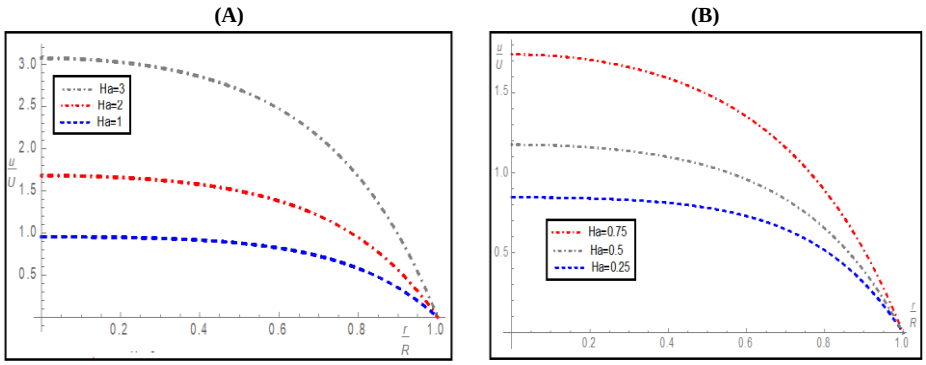

Fig. 3: Variation of Velocity Distribution with R/R for Different Value of Hartmann Number and Da=0.1,S=10,G=-1,B=0.5,K=4.

The impact of Hartmann number on velocity distribution is analyzed in Fig. 3 in the presence of the applied lateral electrical field (S=10). It is interesting to note that velocity at fixed point decreases by increasing the value of Hartmann Number, Ha. This phenomenon is having the same trends for low Hartmann number (see 3. (b)) and also a high magnetic parameter (see Fig 3(a)). The applied magnetic field creates the Lorentz which causes the retarding effect to opposing fluid particle velocity. So, by increasing the applied magnetic field, the development length of Casson fluid flow decreases and for the large value of Hartmann Number and also a low value of Hartmann Number. Fig. 4 (a) and 4. (b) display the variation of velocity distribution by changing the magnetic strength (low and large) when the applied lateral transverse electrical force (S=0). It is interesting the note that in the presence of the lateral electrical field, fully developed length of velocity profiles is more than absent of lateral electric force. Therefore, it is concluded from the above observation that applied a lateral electric field, the velocity of Casson fluid can be controlled. So, the flow rate inside the porous circular microtube can be controlled by combined applying suitable magnetic and lateral electrical force.

Fig. 5 depicts the effect of the Casson parameter on velocity profiles for different when the applied lateral electric field is absent but the presence of the axial electric field. It is noticed that velocity at point increases with increasing the Casson parameter β. The interesting results are to be noted from the fact that the development length of flow is changing by variation Casson parameter β. Fig. 6 shows the effect of Darcy number on velocity profiles. It is noted that velocity is decreasing by increasing the Darcy number that indicates the changing of the permeability of the medium.

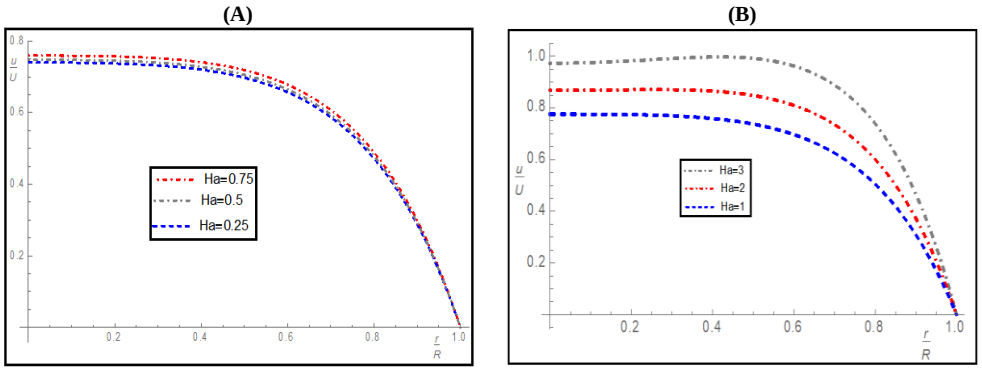

Fig. 4: Variation of Velocity Profiles with R/R for Different Value of Hartmann Number When S=0.

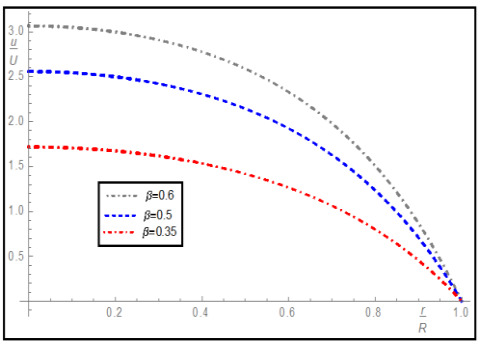

Fig. 5: Variation of Velocity Distribution for Different Values of the Casson Parameter.

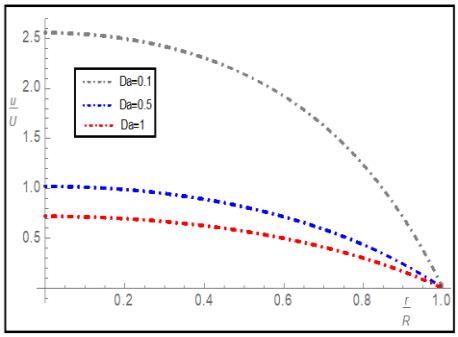

Fig. 6: Variation of Velocity Distribution for Different Values of Darcy Number.

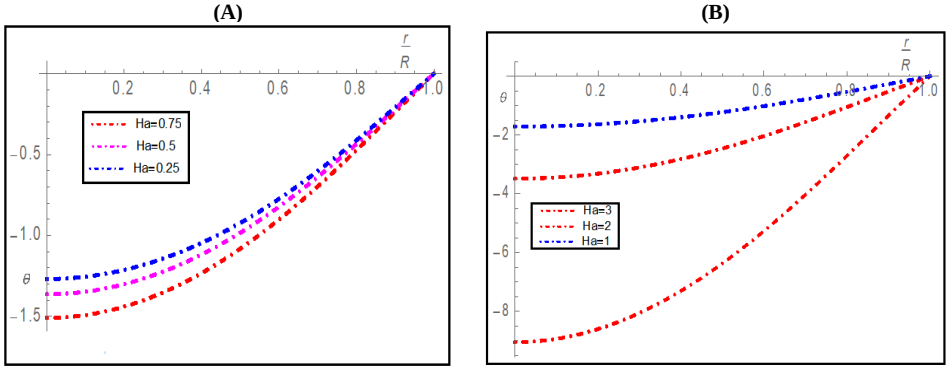

Fig. 7: Variation of Temperature Distribution with R/R for Different Values of Hartmann Number and S_1=1, Da=0.1, Ψ_w^*=-1,S=10,G=-1,B=0.5,K=4, Br=0.01.

Fig. 7 shows the effect of the magnetic parameter (Ha) (Low and high) on temperature distribution in the presence of axial and lateral electrical force components. It is found that the temperature at a point decreases by increasing the applied magnetic field. We can analyze the effect of Darcy number on Temperature distribution from Fig 8. It is pointed out that temperature drops with increasing the Darcy number as the permeability of the medium changes. It is more interesting to the effect of the rate of heat transfer phenomena, and it can be

controlled by changing the Darcy number. Fig 9. shows the variation of the Casson parameter on temperature distribution. It can be remarked from the fact that temperature at a fixed point increases with increasing the Casson parameter.

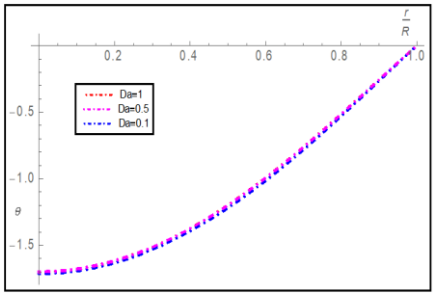

Fig. 8: Variation of Temperature Distribution with R/R for Different Values of Darcy Number.

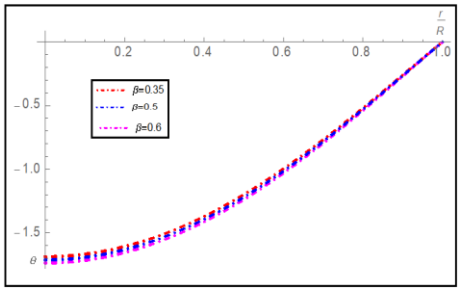

Fig. 9: Variation of Temperature Distribution with R/R for Different Values of Casson Parameter.

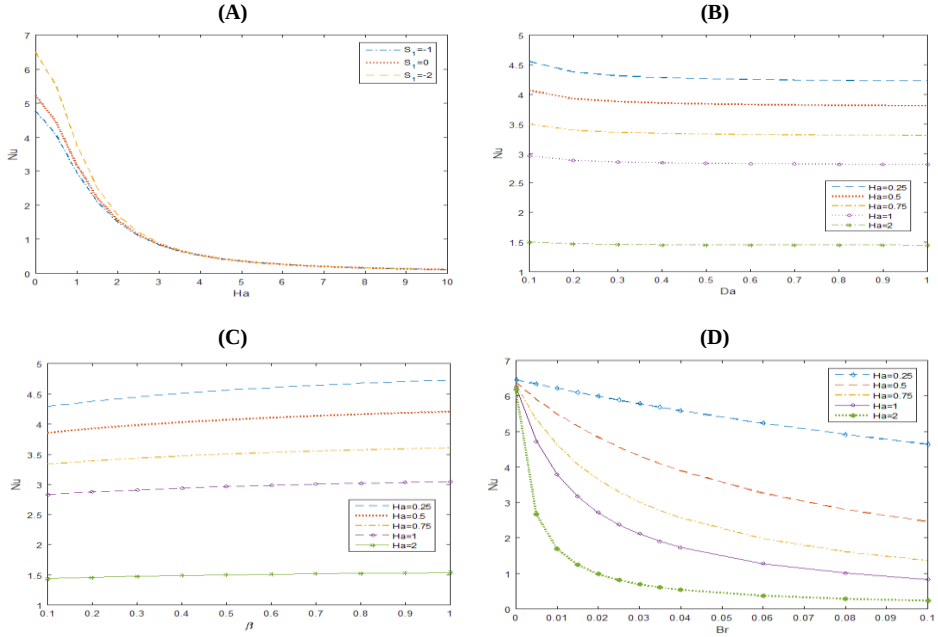

Fig. 10: Variation of Nusselt Number with Hartmann Number, Darcy Number, Casson Parameter, and Brinkman Number.

It is observed that the variation of Nusselt number with various parameter values which are shown in figure 10. Figure 10(a) depicts that the Nusselt number is decreasing with an increase in the strength of the magnetic parameter (Ha). It is noted that the when joule heating parameter is negative then the Nusselt number is increasing. The Nusselt number is decreasing with the increase of Darcy number which represented in figure 10(b). It can be easily seen that when Da is small, the small value of the Hartmann number will result in large Nu. Figure 10(c) delineates that the variation of Nusselt number with the Casson parameter (β) for different values of Hartmann number. It is depicted that the Nusselt number is increasing with the increases of β. It can also be seen that the Nusselt number is large when Ha is small. Figure 10(d) reveals that the variation of Nusselt number with the Brinkman number for different values of Hartmann number. The Nusselt number shows a decreasing trend with the increase in Br for different values of Ha. However, for the large value of the Hartmann number, an interesting phenomenon can be seen that Nu decreases rapidly with increases in the strength of the magnetic field.

4. Conclusions

The exact analytical solutions of velocity and temperature profiles for non-Newtonian Casson fluid in porous microtube under electrokinetic associated with the external magnetic field have been obtained.

- The interesting results are noted that the flow rate inside the porous circular microtube and rate of heat transfer can be controlled by the combined interaction of the electric double layer and applied a magnetic and electric field.
- It is a remarkable observation of the impact of the Casson parameter on velocity and temperature distribution.

- Temperature and velocity distribution depend on Darcy numbers as decreasing the Darcy number flow resistivity increases. Fluid flow becomes slow and the temperature is also increased.
- The Nusselt number is inversely proportional to the Hartmann number, Brinkman number, and Darcy number respectively, but it is proportional to the Casson parameter.
- Another interesting phenomenon is that the Nusselt number is deceased rapidly with the increases of Hartmann number and increases of the Brinkman number for a large value of the strength of the magnetic field.

Acknowledgement

This work was supported by SERB, Govt of India (Grant File No. EMR/2016/006383). The authors would like to acknowledge this support.

References

[1] M. J. Heller, An active microelectronics device for multiplex DNA analysis. IEEE Eng. Med. Biol., 15, (1996) 100– 103. https://doi.org/10.1109/51.486725.
[2] R. G. Sosnowski, E. Tu, W. F. Butler, J. P. O'Connell, M. J. Heller, Rapid determination of single-base mismatch mutations in DNA hybrids by direct electric field control. Proc Natl AcadSci U S A. Feb 18;94(4), (1997) 1119–1123. https://doi.org/10.1073/pnas.94.4.1119.
[3] X. Xuan.; D. Li. Joule heating effects on peak broadening in capillary zone electrophoresis J. Micromech. Microeng. 14 (8), (1997) 1171– 1180. https://doi.org/10.1088/0960-1317/14/8/008.
[4] S Das, T Das, S Chakraborty, Modeling of coupled momentum, heat, and solute transport during DNA hybridization in a microchannel in the presence of electro-osmotic effects and axial pressure gradients, Microfluidics and Nanofluidics 2 (1), (2006) 37-49. https://doi.org/10.1007/s10404-005-0052-9.
[5] J. Jang, S. S. Lee, Theoretical and experimental study of MHD (magnetohydrodynamic) micropump, Sensors Actuators A: Phys., Vol. 80, (2000) 84-89. https://doi.org/10.1016/S0924-4247(99)00302-7.
[6] G. H. Tang, P.X. Ye, W. Q. Tao. Pressure-driven and electroosmotic non-Newtonian flows through microporous media via lattice Boltzmann method, J. Non-Newtonian Fluid Mech. 165, (2010) 1536–1542. https://doi.org/10.1016/j.jnnfm.2010.08.002.
[7] C. Zhao, C Yanga, Electro-osmotic mobility of non-Newtonian fluids Biomicrofluidics 5, (2011) 014110. https://doi.org/10.1063/1.3571278.
[8] A. J. Chamkha, Flow of two-immiscible fluids in porous and nonporous channels J. Fluids Eng. 122(1), (2000) 117-124 https://doi.org/10.1115/1.483233.
[9] A. J. Chamkha, Hydromagnetic two-phase flow in a channel, International Journal of Engineer-ing Sciences, 33(3), (1995) 437-446. https://doi.org/10.1016/0020-7225(93)E0006-Q.
[10] A. J. Chamkha, M. Molana, A. Rahnama, F. Ghadami, On the nanofluids applications in micro-channels: a comprehensive review, Powder Technol-ogy, 332, (2018) 287-322. https://doi.org/10.1016/j.powtec.2018.03.044.
[11] A. J. Chamkha, Unsteady hydromagnetic natural convection in a fluid-saturated porous medium channel, Advances in Filtration and Separation Technology, 10, (1996) 369-75.
[12] A. J. Chamkha, Non-Darcy fully developed mixed convection in a porous medium channel with heat generation/absorption and hydromagnetic effects, Numerical Heat Transfer, 32, (1997) 653-75 https://doi.org/10.1080/10407789708913911.
[13] H. A. Attia, M. E. Sayed-Ahmed, Transient MHD couette flow of a Casson fluid between parallel plates with heat transfer," Italian Journal of Pure and Applied Mathematics, 27, (2010) 19–38. https://doi.org/10.4236/eng.2011.31005.
[14] S. A. Shehzad, T. Hayat, M. Qasim, S. Asghar, Effects of mass transfer on MHD flow of Casson fluid with chemical reaction and suction, Brazilian Journal of Chemical Engineering, 30, (2013) 187–195. https://doi.org/10.1590/S0104-66322013000100020.
[15] M. Afikuzzaman, M. Ferdows, M. M. Alam, Unsteady MHD casson fluid flow through a parallel plate with hall current," Procedia Engineering, 105(2015) 287–293. https://doi.org/10.1016/j.proeng.2015.05.111.
[16] J. R. Buchanan, C. Kleinstreuer, J.K. Comer, Rheological effects on pulsatile hemodynamics in a stenosed tube, Comput. Fluids 29, (2000 695-724 https://doi.org/10.1016/S0045-7930(99)00019-5.
[17] S. Chakravarty, Effects of stenosis on the flow-behavior of blood in an artery, Int. J. Eng. Sci. 25, (1987) 1003-1016. https://doi.org/10.1016/0020-7225(87)90093-0.
[18] Y. I. Cho, K.R. Kensey, Effects of the non-Newtonian viscosity of blood on flows in a diseased arterial vessel. Part 1: Steady flow, Biorheology 28, (1991) 241-262 https://doi.org/10.3233/BIR-1991-283-415.
[19] D. N. Ku, Blood flow in arteries, Annu. Rev. Fluid Mech. 29, (1970) 399-434. https://doi.org/10.1146/annurev.fluid.29.1.399.
[20] R. K Dash, K.N. Mehta, G. Jayaraman, Casson fluid flow in a pipe filled with a homogeneous porous medium, Int. J. Eng. Sci. 34, (1996) 1145-1156. https://doi.org/10.1016/0020-7225(96)00012-2.
[21] M. Liu J. Yang, Electrokinetic effect of the endothelial glycocalyx layer on two-phase blood flow in small blood vessels, Microvasc Res,78(1), (2009) 14-9. https://doi.org/10.1016/j.mvr.2009.04.002.
[22] M. Liu, Q. Guo, J. Yang, Modeling of electroosmotic pumping of non-conducting liquids and biofluids by a two-phase flow method, Journal of Electroanalytical Chemistry, 636, (2009) 86-92. https://doi.org/10.1016/j.jelechem.2009.09.015.
[23] C. Ng, Combined pressure-driven and electroosmotic flow of Casson fluid through a slit microchannel, Journal of Non-Newtonian Fluid Mechanics, 198. (2013) 1-9. https://doi.org/10.1016/j.jnnfm.2013.03.003.
[24] X. Chen, Y. Jian, Z. Xie, Z. Ding, Thermal transport of electromagnetohydrodynamic in a microtube with electrokinetic effect and interfacial slip, Colloids and Surfaces A: Physicochemical and Engineering Aspects, 540, 5, (2018),194-206. https://doi.org/10.1016/j.colsurfa.2017.12.061.
[25] K. Wang, F. Tavakkoli, S. Wang, K.Vafai, Forced convection gaseous slip flow in a porous circular microtube: An exact solution, International Journal of Thermal Sciences, 97, (2015) 152-162. https://doi.org/10.1016/j.ijthermalsci.2015.06.003.
[26] A. M. Afonso, M. A. Alves. T. Pinho FT, Analytical solution of two-fluid electroosmotic flows of viscoelastic fluids, J. Colloid Interface Sci. 395, (2013), pp.277–286. https://doi.org/10.1016/j.jcis.2012.12.013.
[27] G. P. Zhao, Y. J. Jian, F. Q. Li, Streaming potential, and heat transfer of nanofluids in microchannels in the presence of the magnetic field, J. Magn. Magn. Mater. 407, (2016) 75–82. https://doi.org/10.1016/j.jmmm.2016.01.025.
[28] Y. J. Jian, Transient MHD heat transfer and entropy generation in a micro parallel channel combined with pressure and electroosmotic effects, Int. J. Heat Mass. Transf. 89 (2015 193–205. https://doi.org/10.1016/j.ijheatmasstransfer.2015.05.045.
[29] R. Chakraborty, R. Dey, S.Chakraborty, Thermal characteristics of electromagnetohydrodynamic flows in a narrow channel with viscous dissipation and Joule heating under constant wall heat flux, Int. J. Heat Mass. Transf. 67, (2013) 1151–1162. https://doi.org/10.1016/j.ijheatmasstransfer.2013.08.099.
[30] R F. Probstein, Physicochemical Hydrodynamics (New York: Wiley) (1994). https://doi.org/10.1002/0471725137.